SPATIOMAP generation from SPOT 5 super mode images

B.TAKARLI*, I.BOUKRECH, A.DJILALI, M.HADEID

Centre des Techniques Spatiales, 01 avenue de Palestine
BP 13 Arzew Oran Algeria.
b_takarli@yahoo.fr.

Abstract: The development of the society is directly related to the quality and the accessibility (large distribution) of maps, witch is considered as an important document in several sectors like natural resources exploitation, disaster management, commerce, transportation and many other social interactions are simplified if maps are updated, more detailed and widely distributed.

Here, we review different methods that we used to orthorectify a SPOT 5 Super Mode very high resolution image of ORAN (ALEGERIA). In this application we tested seven geometric models for the orthorectification, and we deduce the applicability of different geometric models for the orthorectification of SPOT 5 images and the reachable accuracy. Finally to present this product for non professional user a pseudo natural colors transformation has been calculated, and a 1:25 000 spatiomap based on the SPOT 5 orthoimage was edited.

Keywords: Orthorectification, Geometric, Modelling, High resolution, SPOT

1 Introduction

In Africa, Algeria is at the 8th place, with a CDI (Cartographic Development Index) of 82.23. Only 350 among 1852 mid-scale maps (1:25.000) exist. In this situation we are obliged to look for an alternative to the aerial photographs. The very high resolution satellites have an important impact in the geoinformatic industry. By means of this technology, detailed maps in multiple scales can be frequently and easily generated or updated from images with a gain in cost and time of the operations.
Before, the only solution for medium and large scale maps production was by exploitation of the aerial photography, but at the end of 1999 the very high resolution satellite imagery is commercially available for civil applications, this product is becoming rapidly a real concurrent of the aerial photography.
Many providers of very high resolution satellite images exist and they offer images with a ground sample distance (GSD) from 0.7 to 5 meters, Table 1 shows some very high resolution satellite and their characteristics:

Table 1. Very high resolution satellites [6]

Satellite	Altitude	Swath	Revisit time	GSD
Spot	830 km	60 km	3-26 Day	5 - 2.5m
Eros-a1	480 km	12.5km	3 Day	1.8m
Orbview3	740 km	8 km	1-3 Day	1m
Ikonos	680 km	11 km	1-3 Day	1m
Quickbird	600 km	16 km	1-5 Day	0.61-2.4m

This type of images gives us all the advantages of satellite imagery technology like revisit time, it hasn't a geographical or political frontier and relatively low cost …, in the other hand different problems appear with this new technology such difficulty in the application of classic methods of classification, occlusion, shadow, textural characteristic of the objects is more important…
All these problems are related to the extraction of information. Before the use of this information for GIS or mapping applications, we must consider the geometric aspect of this new satellite imagery technology.

This is equivalent to give an answer to the question “how the imaging system transforms the location of the pixels on the earth to the image?” (Fig.1).

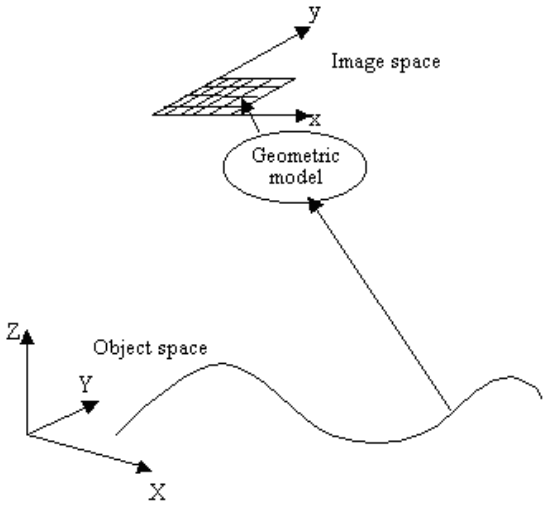

Fig. 1. Geometric modeling.

Several authors were studied this problem, generally we have two categories of geometric models: physical and empirical models. The physical called also rigorous or deterministic models which reflect the physical reality of the viewing geometry (platform, sensor, Earth and sometimes map projection); generally in the optical imagery these models are based on the well-known collinearity condition, which can be considered for each image raw at any time, for the satellite scanner. The empirical, implicit or non parametric models can be used when the parameters of the acquisition systems or a rigorous 3D physical model are not available. Since they do not reflect the source of distortions [7], these models represent the acquisition system as a mathematical transformation between object and image spaces.

2 Rational function model

As an alternative for the physical model, 3D rational functions are widely used as a geometric model for very high satellite images, this approximation of physical model is given as a set of rational polynomials expressing the normalized row and column values, as a function of normalized geodetic latitude, longitude, and height [5],
The rational function polynomial equations are defined as:

$$r = \frac{P_{i1}(X,Y,Z)_j}{P_{i2}(X,Y,Z)_j} \qquad c = \frac{P_{i3}(X,Y,Z)_j}{P_{i4}(X,Y,Z)_j} \qquad \textbf{(1)}$$

Where c, r = image coordinates
X, Y, Z = object coordinates

The rational function polynomial equation numerators and denominators each are 20-term cubic polynomial functions of the form:

$$\begin{aligned} P_{i1}(X,Y,Z) &= a_1 + a_2 \cdot Y + a_3 \cdot X + a_4 \cdot Z \\ &+ a_5 \cdot Y \cdot X + a_6 \cdot Y \cdot Z + a_7 \cdot X \cdot Z + a_8 \cdot Y^2 \\ &+ a_9 \cdot X^2 + a_{10} \cdot Z^2 + a_{11} \cdot X \cdot Y \cdot Z \\ &+ a_{12} \cdot Y^3 + a_{13} \cdot Y \cdot X^2 + a_{14} \cdot Y \cdot Z^2 \\ &+ a_{15} \cdot Y^2 \cdot X + a_{16} \cdot X^3 + a_{17} \cdot X \cdot Z^2 \\ &+ a_{18} \cdot Y^2 \cdot Z + a_{19} \cdot X^2 \cdot Z + a_{20} \cdot Z^3 \end{aligned} \quad \textbf{(2)}$$

Where ai = polynomial coefficients
Y, X, Z = geodetic latitude, longitude, and height

The parameter a1 for the denominators is equal to 1, in order to solve the RF coefficients (78 coefficients); at least 39 control points are required [3].
Space Imaging and DigitalGlobe provide with the image in TIFF format an ASCII file that contains the translation and scale factor used for coordinates normalization and the eighty coefficients. These RPC files (Rational Polynomial Coefficients or Rapid Positioning Capability) are used by the software that supports IKONOS and QUICKBIRD geometric model for georeferencing and the orthorectification. Some other software derives RPC's directly from ephemeris provided with the satellite images and uses the same orthorectification process as IKONOS or QUICKBIRD.
These “intelligent” polynomial functions reflect then better the geometry in both axes and reduce the over-parameterization and the correlation between terms [7].

3 Geometric models

3.1 Direct Linear Transformation

Direct Linear Transformation, known as DLT, it was developed in 1971 by Abdel-Aziz and Karara for close-rang photogrammetry applications. This model can also be used for image rectification [1].
The DLT represents a special case of the Rational Function Model, with first-degree polynomials and common denominators. It can be expressed as:

$$\begin{aligned} r &= \frac{L_1 X + L_2 Y + L_3 Z + L_4}{L_9 X + L_{10} Y + L_{11} Z + 1} \\ c &= \frac{L_5 X + L_6 Y + L_7 Z + L_8}{L_9 X + L_{10} Y + L_{11} Z + 1} \end{aligned} \quad \textbf{(3)}$$

Where c, r = image coordinates
X, Y, Z = object coordinates
L1…L11= DLT parameters

With eleven parameters this model can be solved with 6 points minimum.

3.2 3D Affine Model

This model can be use to express the relationship between object and image coordinates for scanners with a narrow AFOV (Angular Field Of View) and moving with constant-velocity and constant attitude [4].

$$r = L_1X + L_2Y + L_3Z + L_4$$
$$c = L_5X + L_6Y + L_7Z + L_8 \quad \textbf{(4)}$$

It has eight parameters: translation (two), rotation (three), and non-uniform scaling and skew distortion within image space (three). [C.S.Fraser & T. Yamakawa 2003].

3.3 Parallel Perspective Model

Since the acquisition instruments are line scanning systems, a simplification of the DLT which limits the above equation to one line seems to be justified [8].

$$r = \frac{L_5X + L_6Y + L_7Z + L_8}{L_9X + L_{10}Y + L_{11}Z + 1}$$
$$c = L_1X + L_2Y + L_3Z + L_4 \quad \textbf{(5)}$$

This may be interpreted as if the image has the perspective projection in rows (scan line direction) and affine in columns (along-track).

3.4 2D Affine model

When the image area is flat, low-order polynomials can offer good results, in the case of 2D affine transformation the Z coordinate is set to 0 so the expression become:

$$r = L_1X + L_2Y + L_3$$
$$c = L_4X + L_5Y + L_6 \quad \textbf{(6)}$$

3.5 Projective transformation

This transformation describe the projectivity between tow plans [2].

$$r = \frac{L_1X + L_2Y + L_3}{L_7X + L_8Y +}$$
$$c = \frac{L_4X + L_5Y + L_6}{L_7X + L_8Y + 1} \quad \textbf{(7)}$$

The object plane and the image plane do not have to be parallel. 2-D DLT guarantees accurate plane- to-plane mapping regardless of the orientation of the planes. The control points must not be collinear and must form a plane. [9].

4 Experiments

4.1 Overview

The data used in this study is an image of Oran (Algeria) that was acquired at 10:50am local time on April 24th, 2004. A subset has been taken over the area of ARZEW, this subset has a size of 5105*2825 pixels (Fig. 2.), the south of this district is relatively flat, and the northern zone is mountainous with an elevation range from 0 to 310 meters above mean sea level.
A raster DTM used for the orthorectification was been generated form a digitalization of contours from a georeferenced map in 1/25 000 scale, and also 19 Points was been extracted from this map used as control and check points.

Fig. 2. The sub-set over ARZEW.

4.2 Tests and results

The geometric models that we evaluate in this study are: DLT (Direct Linear Transformation), 3D Affine Model, Parallel Perspective Model, 3D SOPM (3D Second -Order Polynomial Model), First Order 3D RFM (Rational Function Model), Plan Projective Model and Plan Affine Model.
The first test is realized with 11 control points and 8 check points (Table 2., Table 3.), although the low redundancy the 3D SOPM and first order RFM give best statistical results.

Table 2. First test results for control points.

	Xmax (pixel)	Xmin (pixel)	Xrms (pixel)	Ymax (pixel)	Ymin (pixel)	Yrms (pixel)
DLT	2.272	0.165	1.361	1.124	0.303	0.786
3D Affine	2.448	0.171	1.252	2.110	0.057	1.212
Parallel	0.841	0.104	0.540	2.110	0.057	1.212
2nd Poly	0.472	0.024	0.264	0.260	0.013	0.145
1st RFM	0.841	0.104	0.540	0.671	0.090	0.399
2D Affine	4.978	0.522	2.715	2.260	0.188	1.530
Plane Proj	3.354	0.099	1.540	2.509	0.136	1.475

Table 3. First test results for check points.

	Xmax (pixel)	Xmin (pixel)	Xrms (pixel)	Ymax (pixel)	Ymin (pixel)	Yrms (pixel)
DLT	4.292	0.557	2.726	2.581	0.055	1.583
3D Affine	3.209	0.393	1.796	2.876	0.256	1.627
Parallel	3.692	0.091	1.862	2.876	0.256	1.627
2nd Poly	1.958	0.151	1.362	2.718	0.214	1.486
1st RFM	3.692	0.091	1.862	1.815	0.657	1.356
2D Affine	4.665	0.070	2.729	2.421	0.166	1.567
Plane Proj	3.979	0.513	2.666	2.719	0.154	1.543

In the second test (Table 4.) we use all the 19 points as control points, the best RMS is given by 3D Second Order Polynomial model (0.7 pixel) and RFM, the projective parallel model gave 0.9 and 1.3 pixels.

Table 4. Second test results in pixel.

	Xmax (pixel)	Xmin (pixel)	Xrms (pixel)	Ymax (pixel)	Ymin (pixel)	Yrms (pixel)
DLT	2.624	0.007	1.712	2.425	0.029	1.055
3D Affine	2.853	0.080	1.460	2.701	0.183	1.316
Parallel	2.160	0.049	0.928	2.701	0.183	1.316
2nd Poly	1.527	0.014	0.711	1.523	0.012	0.659
1st RFM	2.160	0.049	0.928	1.734	0.066	0.785
2D Affine	4.797	0.288	2.643	2.984	0.054	1.466
Plane Proj	3.127	0.018	1.672	2.925	0.120	1.526

In the third test (Table 5.) we use the 19 control points, and same 19 points for check points but we set their elevation as 0, this give us an idea about the influence of z variation in the different models, in this test we deduce that the 3D Second-Order Polynomial model is very sensitive to the variation in elevation, the maximum displacement in points position is 41 and 59 pixels in x and y respectively; The RFM and the perspective parallel model gives 19 pixels in x direction but for y the first give 18 pixels and the second 7 pixels for the same point.

Table 5. Third test results for check points.

	Xmax (pixel)	Xmin (pixel)	Xrms (pixel)	Ymax (pixel)	Ymin (pixel)	Yrms (pixel)
DLT	31.159	0.722	10.492	10.451	0.110	3.385
3D Affine	18.931	0.039	5.549	7.206	0.0002	2.048
Parallel	19.244	0.186	7.397	7.206	0.0002	2.048
2nd Poly	41.233	0.011	14.849	59.698	0.452	20.468
1st RFM	19.244	0.186	7.397	18.931	0.024	8.575

In the final test (Table 6.) we change the latitude and longitude of one of 19 points about 0℃'1" to study the ability of these models to detect the erroneous point; here we can see that all these models are able to detect the erroneous point.

Another test with an error of 0℃'0.5" have been do ne, we note that only first order RFM and DLT permit to detect the erroneous point.

Table 6. Last test results (Dmax is the maximum displacement and Derr is the displacement of the erroneous point).

	Dmax (pixel)	Dmin (pixel)	Dmoy (pixel)	Drms (pixel)	Derr (pixel)
DLT	4.773	0.642	2.035	0.903	4.7734
Affine 3D	5.559	0.465	2.009	1.185	5.5593
Parallel	4.265	0.556	1.707	0.902	4.2654
2nd Poly	3.126	0.093	1.084	0.779	3.1261
1st RFM	3.0591	0.3973	1.2868	0.7410	3.0591
affine 2D	6.5793	0.8295	2.8315	1.6338	6.5793
Plane Proj	4.0104	0.5819	2.0895	0.8902	4.0104

Since the third order 3D FRM is the general case of all the precedent models, the module that calculate each model generate an equivalent RPC file by giving 0 to all the coefficient that must be removed , for example for the second order 3D polynomial all the coefficients of third order terms are set to 0.

This file is loaded with the SPOT5 image as an IKONOS or QUICKBIRD image in images processing software that support these satellites models (RFM).

Both 3D SOPM and first order RFM have been used to generate an orthoimage; a visual inspection and comparison with the map indicate that there is mismatch in some area (Figure 3.); at the time of digitalisation of the contours the coast line was set to 0 where the pier have an elevation of 10 meters, that let as thinking about the DTM precision.

Figure 3. Superimposition with transparency of the map and orthoimage with 3D SOPM.

Another test have been done to observe the influence of the quality of the DTM on the final product; for this we translate all the check points by 10 meters in elevation and recalculate their planimetric positions (Table 7.)

Table 7. Sensitivity of the 3D SOPM to the elevation error.

	3D SOPM		RFM	
	Original (pixel)	After translation (pixel)	Original (pixel)	After translation (pixel)
Max	3.1310	8.2803	3.7498	3.8288
Min	0.9700	0.7391	0.6701	1.2872
Mean	1.8364	3.1137	2.0109	2.5036
RMS	0.7204	2.3351	0.9110	0.8094

4.3 Pseudo-natural color transformation

The pseudo-natural color transformation is used to reconstitute an approximation of natural color visualisation (green vegetation, brown soil …) using the original bands.

As it is known SPOT 5 hasn't the blue band, so the generated Ortho-image is in false colors, this product is not suitable for non professional user. This oblige as to try to find a methodology that allow us to present the final product in pseudo natural colors, this has been done by calculating (using least square method) a transformation between tow spaces, as input the false colors and output the natural color.

The expression of this transformation is:

$$\begin{aligned} PNC_R &= R \\ PNC_G &= G \\ PNC_B &= L_1 * NIR + L_2 * R + L_3 * G \end{aligned} \quad \textbf{(8)}$$

NIR : Near Infra Red value.
R = Red value.
G = Green value.
PNCi = Pseudo-Natural Color (i = R,G,B).

Since the red and green bands are original we need only to calculate the blue one, after a least square transformation we found the coefficients to estimate the blue bands:

$$PNC_B = -0.21*NIR - 0.095*R + 0.7*G \quad \textbf{(9)}$$

This color transformation is realized under ERDAS modeler (Fig. 4.)

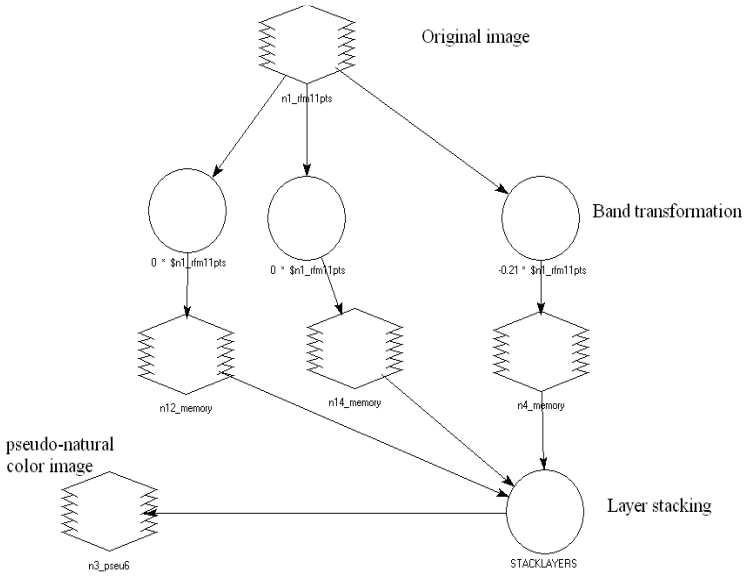

Fig 4. The workflow chart of the Pseudo-natural color transformation

The resulted orthoimage is edited and presented in Fig. 5.

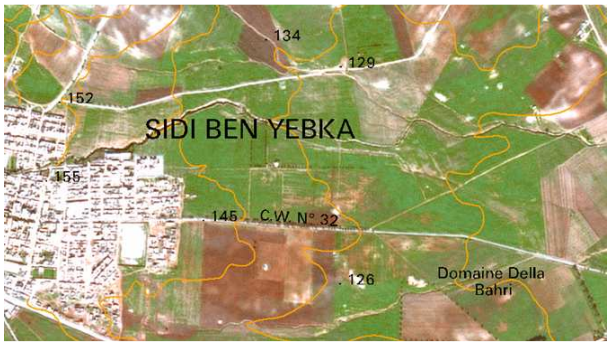

Fig 5. A part of the pseudo-natural color orthoimage after edition.

5 Conclusion

This paper present the accuracy achievable using different geometric models to orthorectify SPOT 5 image, we note that:

The parallel projective model gave better results than the 3D affine and DLT model.
The second order 3D polynomial and first order 3D RFM are better but we must have at least 10 and 8 points uniformly distributed over the image.
The 2D affine and projective transformation gives an interesting since we haven't to measure the elevation of the points and DTM.
The second order 3D polynomial is the most sensitive to the variation in elevation so the DTM to be used must be more accurate.
The pseudo-natural color transformation allows the non accustomed (professional) users the possibility of direct interpretation which facilitate the use of the orthoimage.

Future work will be focused on more detailed study for geometric modeling using large images and bundle adjustment. Since the obtained accuracy is interesting the use of this product for cadastral operations in large and desert regions is conceivable.

ACKNOWLEDGEMENTS

The authors thanks, R.MAHMOUDI, A.RACHEDI, D.YOUSSFI and A.TRACH for their help.

References

[1] C. Vincent Tao and Yong Hu. *Use of the rational function model for image rectification*, Canadian Journal of Remote Sensing, 27(6), pp. 593-602, 2001.

[2] H.B. Hanley and C.S. Fraser. *Geopositioning accuracy of ikonos imagery: indications from 2D transformations*. Submitted to Photogrammetric Record, 5 April 2001.

[3] K. Di, R. Ma and R. Li. *Rational Functions and Potential for Rigorous Sensor Model Recovery*, Photogrammetric Engineering & Remote Sensing, Revised in April 2002.

[4] M. Morgan. *Epipolar Resampling of Linear Array Scanner Scenes*, PHD Thesis, University Of Calgary, 2004.

[5] NIMA. *The Compendium of Controlled Extensions (CE) for the National Imagery Transmission Format (NITF),* version 2.1, 16 November 2000.

[6] A.Puissant. *Information géographique et images a très haute résolution, utilité et applications en milieu urbain*, Luis Pasteur University, France.

[7] T.Toutin. *Review paper: Geometric processing of remote sensing images: Models, Algorithms and Methods*, 2003.

[8] Vozikis, G., Fraser, C., Jansa. *Alternative sensor orientation models for high resolution satellite imagery*. Band 12 " Publikationen der Deutschen Gesellschaft für Photogrammetrie, Fernerkundung und Geoinformation" Bochum (2003), pp. 179- 186.

[9] Y.H Kwon. *Camera Calibration. The DLT method* http://kwon3d.com/theory/dlt/dlt.html#2d (accessed 05 Nov. 2008).